Impaired endochondral ossification and angiogenesis in mice deficient in membrane-type matrix metalloproteinase I

Zhongjun Zhou*, Suneel S. Apte†, Raija Soininen*, Renhai Cao‡, George Y. Baaklini§, Richard W. Rauser§, Jianming Wang¶, Yihai Cao‡, and Karl Tryggvason*‖

*Division of Matrix Biology, Department of Medical Biochemistry and Biophysics, Karolinska Institutet, S-171 77 Stockholm, Sweden; †Department of Biomedical Engineering, Lerner Research Institute, Cleveland Clinic Foundation ND-20, 9500 Euclid Avenue, Cleveland, OH 44195; ‡Microbiology and Tumor Biology Center, Karolinska Institutet, S-171 77 Stockholm, Sweden; §Glenn Research Center, Life Prediction Branch, National Aeronautics and Space Administration, Cleveland, OH 44135; and ¶Department of Molecular Medicine, Karolinska Hospital, S-171 76 Stockholm, Sweden

Communicated by Darwin J. Prockop, MCP Hahnemann University, Philadelphia, PA, January 28, 2000 (received for review November 30, 1999)

Membrane-type matrix metalloproteinase I (MT1-MMP)-deficient mice were found to have severe defects in skeletal development and angiogenesis. The craniofacial, axial, and appendicular skeletons were severely affected, leading to a short and domed skull, marked deceleration of postnatal growth, and death by 3 wk of age. Shortening of bones is a consequence of decreased chondrocyte proliferation in the proliferative zone of the growth plates. Defective vascular invasion of cartilage leads to enlargement of hypertrophic zones of growth plates and delayed formation of secondary ossification centers in long bones. In an *in vivo* corneal angiogenesis assay, null mice did not have angiogenic response to implanted FGF-2, suggesting that the defect in angiogenesis is not restricted to cartilage alone. In tissues from null mice, activation of latent matrix metalloproteinase 2 was deficient, suggesting that MT1-MMP is essential for its activation *in vivo*.

Matrix metalloproteinases (MMPs) are a family of Zn-dependent enzymes that are essential for extracellular matrix (ECM) turnover in normal and pathological conditions (1, 2). The MMPs are produced as latent proenzymes, and can be inhibited by specific tissue inhibitors of metalloproteinases (TIMPs). The enzymes can be divided into two structurally distinct subgroups, i.e., membrane-type (MT-MMP) and secreted MMPs. The secreted MMPs include interstitial collagenases (MMP-1, -8, and -13), which degrade fibrillar collagens, gelatinases (type IV collagenases, MMP-2 and -9) with high activity against gelatin and type IV collagen, and stromelysins (MMP-3, -10, and -11), which degrade a variety of collagenous and noncollagenous ECM proteins. Although the secreted MMPs have different expression patterns, there seems to be considerable redundancy and overlap between them with respect to function. Thus, mice deficient for MMP-2 (3), MMP-3 (4), MMP-7 (5), MMP-9 (6), MMP-10 (7), or MMP-12 (8) are all viable. Of these, only the MMP-9-deficient mice have been reported to show developmental abnormalities, which involve the growth plate and endochondral ossification (6).

To date, five genetically distinct MT-MMPs (*Mmp*14–17, *Mmp* 21) have been identified (9–14). These enzymes (except MMP-17, which is glycosylphosphatidylinositol anchored) are single-pass type I membrane proteins with an extracellular N terminus containing the catalytic domain and a short C-terminal cytoplasmic domain. The prototypic MT-MMP, MT1-MMP (also termed MMP-14), was first identified as a cellular receptor and activator for pro-MMP-2 (9), but both MT1-MMP and MT2-MMP (MMP-15) have also been shown to have activity against a variety of ECM proteins, including gelatin, fibronectin, vitronectin, fibrillar collagens, and aggrecan (15, 16). MT1-MMP is widely expressed in cultured cells and tissues during development (17), but its strictly regulated spatial and temporal expression indicates more specific roles for this enzyme (17, 18). A crucial role for MT1-MMP for bone growth was recently demonstrated in MT1-MMP-deficient mice, which have severe defects in skeletal development leading to early death (19). MT1-MMP has also been implicated in neovascularization and angiogenesis processes through its effect on pericellular fibrinolysis (20).

To define the biological role of MT1-MMP, we have generated MT1-MMP-deficient mice by gene targeting in embryonic stem (ES) cells. The mice exhibit severe defects in skeletal development and die by about 3 wk of age. Vascularization of chondroepiphyses is severely impaired, leading to delayed ossification of secondary ossification nuclei. A corneal angiogenesis assay revealed complete absence of neovascularization in the mutant mice in response to fibroblast growth factor (FGF)-2, whereas intensive angiogenesis was observed in wild-type animals. The results indicate an essential role for MT1-MMP in the processes of angiogenesis, in addition to its role in bone growth. Our studies also demonstrated that *in vivo* MT1-MMP is required for activation of pro-MMP-2.

Materials and Methods

Gene Targeting and Generation of Transgenic Mice. A 0.5-kb *Stu*I fragment was excised from a genomic MT1-MMP clone and replaced by a neomycin cassette with the *pgk1* promoter (Fig. 1*A*). A *hsv*-thymidine kinase cassette, also driven by the *pgk1* promoter, was placed at the 3′ end of the construct. The targeting construct was introduced into RW4 ES cells by electroporation, followed by G418 and gancyclovir double selection. Homologous recombination targeting events were identified in seven of 350 ES cell colonies (Fig. 1*B*). Two clones were used for injections into blastocysts of C57BL/6 mice, one of these giving germ-line transmission. Homozygous null mice were generated by heterozygote mating, and heterozygotes were crossed back to the C57BL/6 strain. A stable phenotype has been observed in mice backcrossed for five generations.

High-Resolution Radiography. A modularized, digital x-ray imaging system (SMARTSCAN Model 112; Scientific Measurement Systems, Austin; TX) using a microfocus x-ray source (FEINFOCUS FXE160) was used to produce very high-resolution imaging of bone samples, approaching 25 μm (about 1 mil) in the

Abbreviations: MMP, matrix metalloproteinase; MT-MMP, membrane-type MMP; TIMP, tissue inhibitor of metalloproteinase; ECM, extracellular matrix; FGF, fibroblast growth factor; ES, embryonic stem; PECAM, platelet endothelial cell adhesion molecule; VEGF, vascular endothelial growth factor.

‖To whom reprint requests should be addressed. E-mail: karl.tryggvason@mbb.ki.se.

The publication costs of this article were defrayed in part by page charge payment. This article must therefore be hereby marked "*advertisement*" in accordance with 18 U.S.C. §1734 solely to indicate this fact.

Article published online before print: *Proc. Natl. Acad. Sci. USA*, 10.1073/pnas.060037197. Article and publication date are at www.pnas.org/cgi/doi/10.1073/pnas.060037197

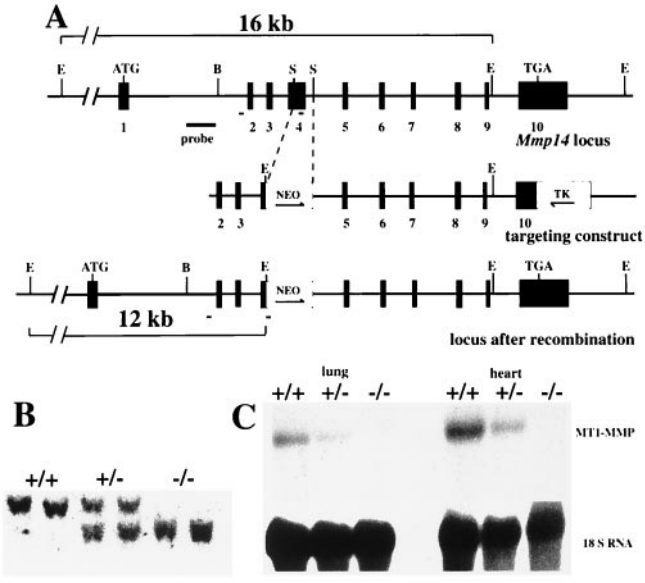

Fig. 1. Targeted inactivation of the MT1-MMP gene. (*A*) 5′ region of the wild type (*Top*), targeting construct (*Middle*), and the gene region after the targeting event. Exons are shown as black boxes and numbered. Directions of the *neo* and *tk* genes (open boxes) are depicted by arrows. The probe used for Southern blots and the location of primers used for PCR (short solid lines) are indicated. E, *Eco*RI; S, *Stu*I; B, *Bam*HI. (*B*) Southern blot analysis of *Eco*RI-digested DNA from a litter generated by F_1 heterozygote mating. The wild-type fragment is 16 kb, and the mutant one is about 12 kb. (*C*) Northern blot analyses of RNA isolated from wild-type and null mouse lung and heart tissues. The filter was hybridized with an MT1-MMP cDNA probe, a probe for 18S RNA being used as a control for RNA loading and integrity.

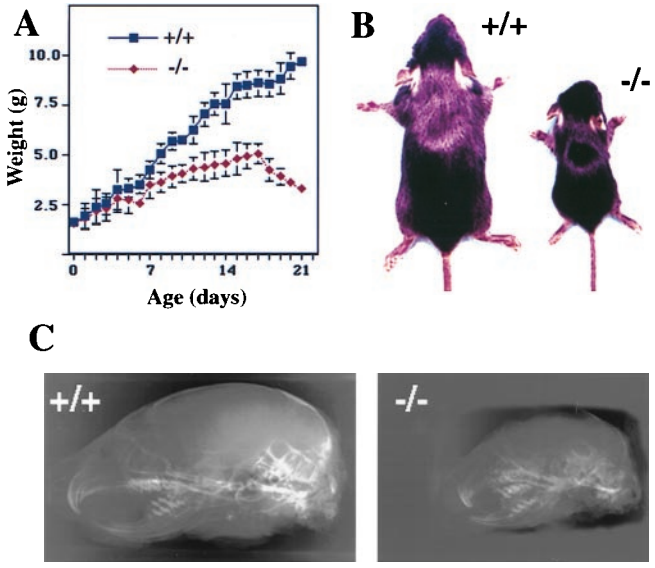

Fig. 2. Retarded growth and cranial deformation in MT1-MMP-deficient mice. (*A*) Growth chart of $-/-$ and $+/+$ mice demonstrates dramatic retardation in the growth of the $-/-$ mice, showing a decrease in body weight during the last days of life. (*B*) Size difference of two $+/+$ and $-/-$ male littermates at age 3 wk. (*C*) Lateral high-resolution radiographs of skulls of $+/+$ and $-/-$ mice at age 2 wk.

computerized tomography mode of operation and 10 μm in the digital radiography mode.

Morphology, Histology, and *in Situ* Hybridization Analyses. Overview of the skeletal system was obtained by staining cleared specimens of the mouse skeleton with Alizarin red S and Alcian blue. For histochemical or immunohistological staining, tissues were fixed in 10% neutral buffered formalin and decalcified in either EDTA or 10% (vol/vol) formic acid. Paraffin sections of 7 μm were stained with hematoxylin and eosin, Masson trichrome, or a modification of the Movat pentachrome stain. Polyclonal antibody against TRAP was a kind gift from Göran Andersson (Huddinge Hospital, Huddinge, Sweden). Antibodies against platelet endothelial cell adhesion molecule (PECAM) and vascular endothelial growth factor (VEGF) antibodies were from Zymed Laboratories, PharMingen and Santa Cruz Biotechnology, respectively.

For *in situ* hybridization, long bones of different stages were dissected and fixed in 4% neutral PBS-buffered paraformaldehyde and decalcified in EDTA solution for 2 wk at 4°C. Specific probes were generated by PCR (21) so that sense primers were flanked by a SP6 promoter sequence and antisense primer was flanked by T7 promoter sequence. The RNA probes were labeled with the Dig RNA Labeling System (Roche Molecular Biochemicals), and hybridizations were carried out as previously described (22).

Gelatinase Activity Assay. Assays for gelatinolytic activity were carried out essentially as previously described (18). Briefly, tissues were homogenized in cold cell lysis buffer [1% Triton X-100/0.1% SDS/50 mM Tris·HCl (pH 7.5)] containing a protease inhibitor mixture. The lysate was incubated on ice for 30 min and centrifuged 8,000 rpm for 15 min at 4°C. Protein samples of 5 μg were separated by 10% PAGE containing 0.2% gelatin. The gel was then incubated in 2.5% Triton X-100 for 1 h and incubated in the reaction buffer [50 mM Tris·HCl (pH 7.5)/5 mM $CaCl_2$/0.2 M NaCl) for 14 h at 37°C. The gelatinase activity was then detected by staining the gel with Coomassie blue and subsequent destaining to visualize the zymogen bands.

Mouse Corneal Micropocket Assay. The mouse corneal assay was performed as previously described (23, 24). Corneal micropockets were created with a modified von Graefe cataract knife in the right eye of each 15-day-old MT1-MMP mutant mouse ($n = 5$) and wild-type littermates ($n = 5$). A micropellet (0.35 × 0.35 mm) of sucrose aluminum sulfate coated with hydron polymer type NCC (IFN Sciences, New Brunswick, NJ) containing 80 ng of human FGF-2 was implanted into each pocket. The pellet was positioned approximately 0.7 mm from the corneal limbus. After implantation, erythromycin/ophthalmic ointment was applied to each eye. The corneal neovascularization was examined by a slit-lamp biomicroscope on day 3 after pellet implantation.

Results

Severe Growth Retardation and Early Death in MT1-MMP-Deficient Mice. Following mating of heterozygotes, MT1-MMP-deficient ($-/-$), heterozygote ($+/-$), and wild-type ($+/+$) mice were obtained in the expected Mendelian ratio. Homozygosity for the inactivated allele was demonstrated by Southern blot (Fig. 1*B*), and the lack of functional MT1-MMP was demonstrated by the absence of MT1-MMP mRNA by using total RNA from lung and heart of 10-day-old mice (Fig. 1*C*).

Heterozygous mice were morphologically indistinguishable from the wild-type littermates, and they had comparable weight, growth rates, and external appearance (data not shown). In contrast, null mice could be distinguished at birth from wild-type littermates by a slightly domed shape of the skull and a short snout, as well as by visually prominent suture lines in the cranium. These subtle changes were the only manifest phenotype at birth when null, heterozygous, and wild-type mice were roughly of the same size and weight (Fig. 2).

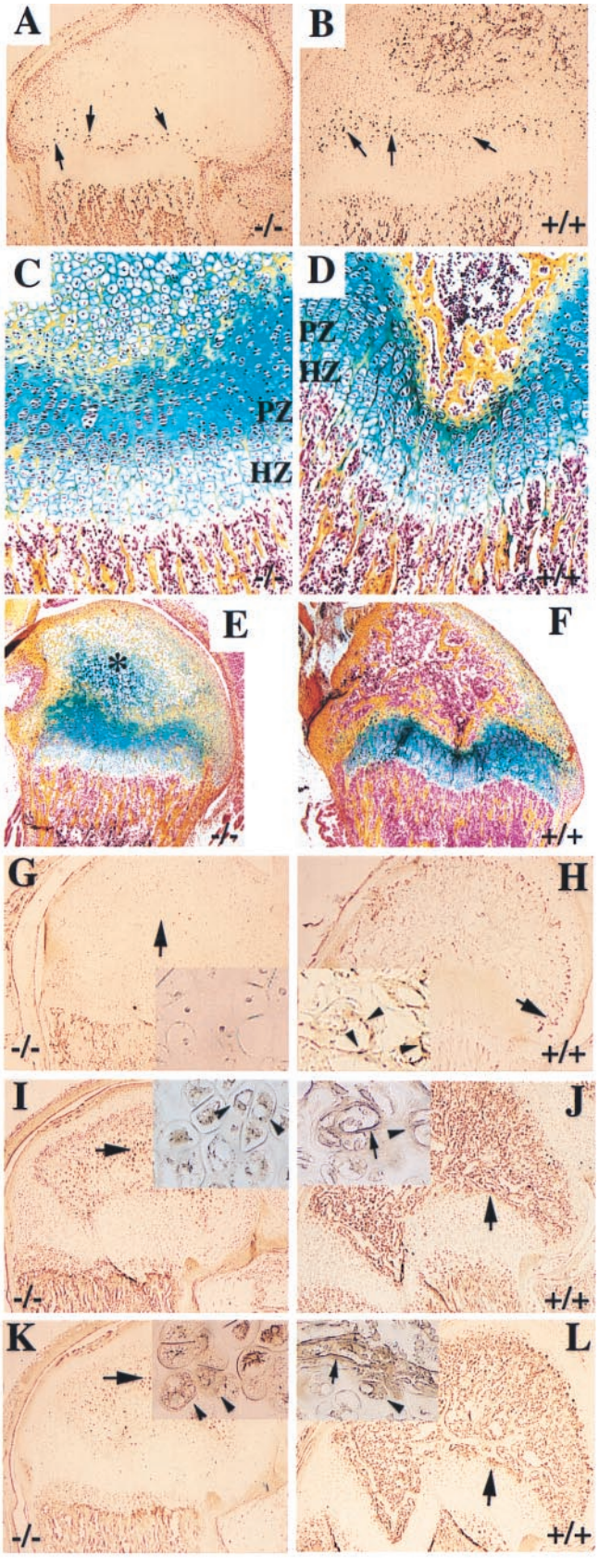

Fig. 3. Histology and immunohistology of growth zones in distal femur. (*A* and *B*) Immunodetection of BrdUrd-labeled cells (brown dots) with lower amount of proliferative cells in the proliferative zone (arrows) of 2-wk-old −/− mice, compared with those of wild-type littermates. (*C* and *D*) Comparative histology of growth plates of the distal femur in 15-day-old mutant (−/−) and in wild type (+/+). Note the disorganized structure and low cell number in the proliferative zone in −/− mice. The lack of vascularization and bone formation in the epiphyseal secondary ossification center of mutant mice can also be observed. (*E* and *F*) Comparison of secondary ossification center of the distal femur from 15-day-old mice. There is advanced ossification in wild-type mice (*F*), whereas hypertrophic chondrocytes persist in the location of the ossific center (∗) of −/− mice, with no signs of ossification (*E*). (*C*–*F*) Modified Movat pentachrome stain; PZ, = proliferative zone; HZ, hypertrophic zone. (*G* and *H*) Immunohistochemical staining with antibodies against PECAM revealing lack of endothelial cells in the epiphysis of −/− mice (*G*), whereas positive staining is seen throughout the epiphysis in controls, as shown to be located in endothelial cells of blood vessels (*G*, *Inset*). Note the similar PECAM staining at the chondroosseous junction in mutant and control mice. Arrows indicate areas magnified in insets. Arrowheads in the insets depict blood vessels (*H*). VEGF (*I* and *J*) and its receptor Flk-1 (*K* and *L*) reveal no evidence for vascularization in the secondary ossification zone of the femoral epiphysis in mutant mice. Insets in *G*–*L* show higher magnifications taken from locations shown by arrows. Arrowheads in insets of *I*–*L* indicate VEGF or Flk-1-positive cells, and arrows in the insets depict the positively stained blood vessels.

The altered craniofacial features, as well as deceleration of linear growth (Fig. 2*A*) were obvious from 3 to 4 days after birth. Subsequently, the craniofacial dysmorphosis, as well as the size difference between null mice and heterozygous or wild-type mice became dramatically obvious. It was most marked immediately before death of null mice around 3 wk of age, when they only had 30–40% of the body weight of wild-type mice (Fig. 2 *A* and *B*). From 1 wk after birth, the null mice were less active and had lax skin. They suffered from wasting and could not be successfully weaned.

Abnormal Skeletal Growth in MT1-MMP-Deficient Mice. An overall survey of skeletal structure and patterning of the MT1-MMP-deficient mice revealed skeletal changes essentially as those described by Holmbeck *et al.* (19). At birth, only minor changes were seen in the craniofacial skeleton (not shown). At later ages, cleared preparations of the head of null mice showed more specific anatomical alterations, such as smaller skull bones and lack of bony coverage of the region between the two parietal and the interparietal bones (not shown). The skull defect has been described in detail by Holmbeck *et al.* (19) and is not discussed further here. All bony elements in the appendicular and axial skeletons of the null mice were proportionately reduced in size relative to wild-type and heterozygous mice (not shown). Thus, the bones were markedly shorter and thinner, but otherwise they displayed normal anatomical features.

High-resolution digital radiography and computerized tomography (CT) of the heads of 2-wk-old wild-type and null mice revealed that the null mice have a significantly shorter craniofacial skeleton. This is because of shortening of the mandible and maxilla and the bones of the base of the skull (Fig. 2*C*). Upper and lower incisors are short, and the upper incisor is curved inward, resulting in malocclusion. The cranial cavity is significantly smaller and the vertex region shows no mineralization. CT scans emphasized the relative lack of mineralization in the null mice (data not shown).

Defects in the Growth Plate and in Endochondral Ossification in MT1-MMP-Deficient Mice. In 16.5-day-old null embryos, longitudinal sections through long bones demonstrated a 3- to 4-fold increase in the thickness of the hypertrophic zone, with no anomaly being visible elsewhere in the growth plate (not shown). The enlargement of the hypertrophic zones was subsequently visible, but incrementally smaller throughout postnatal life. Pulse labeling and immunodetection of BrdUrd in 2-wk-old mice revealed significantly decreased cell proliferation in the prolif-

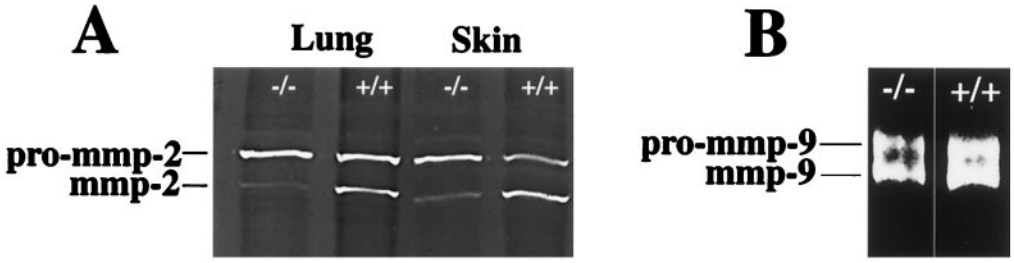

Fig. 4. Gelatinase zymography carried out in SDS/PAGE of tissue extracts from null and wild-type mice reveals decreased *in vivo* activation of pro-MMP-2 (*A*), whereas *in vivo* activation of pro-MMP-9 appears to be unaffected (*B*).

erative zone of the growth plate in null mice as compared with wild-type mice (Fig. 3 *A* and *B*). Furthermore, the proliferative zones of the growth plate became disorganized after age 2 wk in null mice relative to the wild-type mice (Fig. 3 *C* and *D*).

Major defects were also seen in the development and shape of the secondary ossification centers (Fig. 3 *E* and *F*). The secondary ossification centers that form after birth developed poorly in the null mice. For example, at age 2 wk, the secondary ossification nuclei in the distal femur and proximal tibia were absent in the null mice (Fig. 3*E*). Instead, there was a mass of hypertrophic chondrocytes surrounded by chondroid matrix with streaks of osteoid deposition. In contrast to wild-type mice (Fig. 3*H*), no blood vessel formation was visible in the null mice, as shown by lack of staining with antibodies against PECAM (Fig. 3*G*), except at the insertion of the cruciate ligaments where some vascular invasion of the cartilage occurred. Despite the normal expression of VEGF and Flk-1 in hypertrophic epiphyseal chondrocytes, induction of blood vessel invasion failed to occur in the null mice as opposed to their control littermates (Fig. 3 *E–L*).

At the chondroosseous junction, blood vessels and osteoclasts were visible in both wild-type and null mice. Immunostaining with antibodies against PECAM, an endothelial-specific marker, did not show significant differences in the existing blood vessels in terms of density, orientation, or dilation (Fig. 3 *G* and *H*). The structure and composition of the bone marrow appeared to be histologically normal (Fig. 3 *C–F*). Immunostaining with a polyclonal antibody to tartrate-resistant acid phosphatase identified no differences in the number of osteoclasts between null and wild-type mice (data not shown). In both types of mice, osteoclasts were seen adjacent to the last intact transverse septum of the hypertrophic zones. The primary metaphyseal trabeculae appeared normal in size and composition.

The enlarged hypertrophic zone in the growth plates in mutant mice and the fact that MT1-MMP is highly expressed in perichodrium led us to assess whether the absence of the enzyme disturbs the regulation of chondrocyte differentiation and maturation. Expression of several stage-specific bone developmental markers, such as Indian hedgehog, collagens II and X, and PTH receptor, as well as bone morphogenic protein 6, was studied in femora of newborn, 1-wk-old, and 2-wk-old mutant mice and their wild-type littermates by using *in situ* hybridization. The results did not reveal significant differences between mutant and wild-type animals (data not shown).

Impaired Activation of Pro-MMP-2 but Not Pro-MMP-9. Because MT1-MMP has been implicated as an activator of pro-MMP-2 (9), we examined whether activation of the latent form 72-kDa pro-MMP-2 to the active 62-kDa form is decreased in MT1-MMP-deficient mice by using the gelatinolytic assay. As can be seen in Fig. 4*A*, minimal conversion of pro-MMP-2 to its active form occurs in tissue extracts from lung and skin. This indicates that activation of pro-MMP-2 is impaired in the knockout mice, and that MT1-MMP is a major activator of pro-MMP-2 *in vivo*. In contrast, gelatinase assay carried out on bone extract that is high in MMP-9 activity did not reveal any significant differences in the ratios of latent vs. activated forms of MMP-9 (Fig. 4*B*), indicating that MT1-MMP is not important for activation of pro-MMP-9 in bone.

Absence of Corneal Angiogenesis in MT1-MMP-Deficient Mice. The delayed vascularization in the secondary ossification nuclei of long bones in null mice prompted us to explore whether the absence of MT1-MMP affects angiogenesis. To examine this *in vivo*, a corneal micropocket assay was carried out in 2-wk-old mice. Micropellets of aluminum sulfate coated with the slow release polymer-hydron containing human FGF-2 were surgically implanted into the cornea of 15-day-old null mice and their wild-type littermates, and the angiogenic response was examined 3 days later (Fig. 5). In wild-type mice, the limbal vessels were dilated in the FGF-2-implanted corneas. In contrast, FGF-2 was unable to induce angiogenic response in the MT1-MMP-deficient mice. Complete absence of blood vessel growth was observed in all five mice tested until their natural death at around 3 wk of age. The complete absence of FGF-2-induced corneal angiogenesis suggests that MT1-MMP plays a crucial role in the initial step of angiogenesis.

Discussion

Phenotypic analysis of MT1-MMP null mice has recently been reported by Holmbeck *et al.* (19). We independently generated such mice and found similar defects in skeletal development and growth. Here, we also describe additional studies to define a defect in vascular invasion of cartilage, both during endochondral ossification of growth plates and in secondary ossification centers of chondroepiphyses. Furthermore, our studies using an *in vivo* corneal assay demonstrated that this abnormality may be part of a more generalized defect in postnatal angiogenes in MT1-MMP deficiency. The present work also demonstrated that activation of pro-MMP-2 *in vivo* is impaired in the absence of MT1-MMP. Together, the results demonstrate a critical and

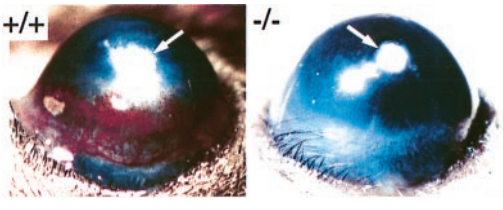

Fig. 5. Corneal neovascularization assay. Three days after implantation, FGF-2 containing pellets angiogenesis is induced in MT1-MMP +/+ mice, whereas no reaction is seen in the cornea of −/− littermates. Arrows point to the implanted pellets.

independent role for MT1-MMP in bone development and angiogenesis, and that MT1-MMP deficiency is incompatible with survival to maturity.

MT1-MMP-Deficient Mice Have Defects in Growth Plates and Delayed Cartilage Resorption During Endochondral Ossification. The MT1-MMP-deficient mice generated in this study had severe defects in skeletal development, resulting in retarded growth. The overall phenotype of the null mice is similar to that recently described by Holmbeck *et al.* (19). However, our mice, that were inbred, always died at age 3 wk, whereas the other null mouse line that was raised in a noninbred background died from 3 to 16 wk of age (19).

The specific enlargement of the hypertrophic zones observed in our null mice is attributable to delayed resorption of cartilage during endochondral ossification. Although wasting may contribute to the bone phenotype postnatally, the enlargement of the growth plate seen in E16.5-day-old humerus and the high expression of MT1-MMP at the chondroosseous junction shown previously (17) and in this study (not shown) clearly indicate a primary function of MT1-MMP in cartilage resorption. Targeted inactivation of *Mmp9* has also been shown to result in enlargement of the hypertrophic zone, but it does not result in retarded growth or craniofacial deformation. Therefore, dwarfism is likely to be the result of defective cell production in the growth plates, as supported by our BrdUrd staining results. Although both MMP-9 and MT1-MMP appear to be independently required for resorption of calcified cartilage at the advancing ossification front, MT1-MMP, but not MMP-9, regulates cell proliferation in the growth plate through an as yet unknown mechanism.

Interestingly, the present results and those of Holmbeck *et al.* (19) showed that the hypertrophic zones in MT1-MMP-deficient mice are not as dramatically enlarged in postnatal life as they are in embryonic bones. This is possibly because of a progressive failure of cell production in postnatal growth plates so that fewer hypertrophic chondrocytes are generated as shown here by BrdUrd labeling. Another possibility is that in postnatal life, other enzymes play a more significant role in cartilage resorption. For example, in *Mmp9* null mice, hypertrophic zone enlargement is seen primarily during a specific temporal window of growth (6). It is also possible that the peak requirement for MMP-9 and MT1-MMP occurs at different ages so that one may partially compensate for deficiencies of the other. These hypotheses can now be tested by crossing *Mmp9* null and MT1-MMP-deficient mice.

The presently generated MT1-MMP-deficient mice have similar severe craniofacial deformations, as reported previously (19). This phenotype is extremely complex, because of the multiple tissues that form it, the complex shapes of the bony components, two different types of ossification (membranous and endochondral), and complex migratory events that bring tissues from different embryonic origins together. Thus, it is difficult to pinpoint the precise defects that lead to the craniofacial anomalies we have described. However, studies in the axial and appendicular skeleton indicate that the growth of craniofacial bones is also likely to be abnormal. Expression of MT1-MMP at high levels in the developing tooth bud may contribute to the altered dentition we have noted, although this may also be the result of retarded mandibular and maxillary development. As a consequence of MT1-MMP inactivation, the cranial cavity is smaller, and like many other mutations affecting skull size, these mice also show a dome-shaped skull and sutural expansion. It is conceivable that the severe facial anomalies of null mice result in malocclusion, which can lead to inefficient feeding and contribution of starvation to the early death of the animals. The malnutrition may also be a contributing factor affecting the longitudinal bone growth.

MT1-MMP Is an *in Vivo* Activator of Pro-MMP-2. Based on *in vitro* studies, MT1-MMP has been implicated in the activation of other pro-MMPs, such as pro-MMP-2, pro-MMP-9, and pro-MMP13 (2, 16, 25). Thus, MT1-MMP binds a complex of pro-MMP-2 and TIMP-2, resulting in the activation of pro-MMP-2. The present data demonstrated a central *in vivo* role for MT1-MMP in the activation of pro-MMP-2, as shown by the fact that the 72-kDa pro-MMP-2 was minimally converted to its active form in tissue extracts such as lung and skin. However, with respect to the phenotype, it is clear that the main role of MT1-MMP is not to serve as an activator of pro-MMP-2 because *Mmp-2* null mice developed normally, whereas MT1-MMP-deficient mice exhibit a severe phenotype. In contrast to MMP-2, the results of this study did not reveal any differences in *in vivo* conversion of pro-MMP-9 to its active form, suggesting that MT1-MMP is not important for activation of pro-MMP-9.

Angiogenesis Is Defective in MT1-MMP-Deficient Mice. The absence of FGF-2-induced angiogenic response in the cornea is an intriguing finding. MMPs have been implicated in the control of angiogenesis both under physiological and pathological conditions, but their precise roles in this process are unclear. The present results demonstrate a direct *in vivo* role of a specific MMP in angiogenesis. It is possible that activation of MMP-2 and possibly other MMPs, such as MMP-13, by MT1-MMP is important for the basement membrane degradation that is required in the initial steps of angiogenesis. However, it cannot be excluded that MT1-MMP itself has a critical role for basement membrane degradation *in vivo*.

The cornea is an avascular tissue and lacks background blood vessels. The complete lack of FGF-2-induced angiogenic response in MT1-MMP-deficient mice indicates that this enzyme is essential in the initiation of angiogenesis, at least in the corneal tissue. A similar defect of angiogenesis may also cause the delayed development of secondary ossification centers and retarded resorption of growth plate cartilage in MT1-MMP null mice. The fact that VEGF expression is not affected in epiphyseal hypertrophic chondrocytes indicates that MT1-MMP is essential for blood vessel invasion into uncalcified cartilage during formation of secondary ossification centers. However, because angiogenesis may also be required in other tissues during embryonic development, the lack of angiogenic response to FGF-2 may not explain why other tissues in the mutant animal developed relatively normally and the mice could survive to the postnatal age of about 3 wk. There are possibly other MMP-independent mechanisms involved in the regulation of the vascular development. Another explanation would be of a tissue-specific effect of MT1-MMP. It is possible that both bone and corneal tissues use MT1-MMP to trigger the angiogenic process, whereas angiogenesis in other tissues is initiated by means of other proteases. A third possibility is that various angiogenic factors induce different proteases to break down the basement membrane of blood vessels. In this case, the angiogenic response of FGF-2 is mediated by means of MT1-MMP, either directly or through activation of pro-MMP-2.

We thank Margaret Bennish, Misty Garcia, Johanna Räisanen, and Minna Pajuportti for expert technical assistance, and Catarina Vibaste for secretarial assistance. This work was supported by funding from the Swedish Cancer Society, European Commission project BMH4-CT 96–0012, Novo Nordisk Foundation, and Hedlund's Foundation (to K.T.), and from the Cleveland Clinic Foundation (to S.A.).

1. Werb, Z. (1997) *Cell* **91,** 439–442.
2. Murphy, G., Stanton, H., Cowell, S., Butler, G., Knauper, V., Atkinson, S. & Gavrilovic, J. (1999) *Acta Pathol. Microbiol. Immunol. Scand.* **107,** 38–44.
3. Itoh, T., Ikeda, T., Gomi, H., Nakao, S., Suzuki, T. & Itohara, S. (1997) *J. Biol. Chem.* **272,** 22389–22392.
4. Mudgett, J. S., Hutchinson, N. I., Chartrain, N. A., Forsyth, A. J., McDonnell, J., Singerm, I. I., Bayne, E. K., Flanagan, J., Kawka, D., Shen, C. F., *et al.* (1998) *Arthritis Rheum.* **41,** 110–121.
5. Wilson, C. L., Heppner, K. J., Labosky, P. A., Hogan, B. L. & Matrisian, L. M. (1997) *Proc. Natl. Acad. Sci. USA* **94,** 1402–1407.
6. Vu, T. H., Shipley, J. M., Bergers, G., Berger, J. E., Helms, J. A., Hanahan, D., Shapiro, S. D., Senior, R. M. & Werb, Z. (1998) *Cell* **93,** 411–422.
7. Masson, R., Lefebvre, O., Noel, A., Fahime, M. E., Chenard, M. P., Wendling, C., Kebers, F., LeMeur, M., Dierich, A., Foidart, J.-M., *et al.* (1998) *J. Cell Biol.* **140,** 1535–1541.
8. Hautamäki, R. D., Kobayashi, D. K., Senior, R. M. & Shapiro, S. D. (1997) *Science* **277,** 2002–2004.
9. Sato, H., Takino, T., Okada, Y., Cao, J., Shinagawa, A., Yamamoto, E. & Seiki, M. (1994) *Nature (London)* **370,** 61–65.
10. Will, H. & Hinzmann, B. (1995) *Eur. J. Biochem.* **231,** 602–608.
11. Takino, T., Sato, H., Shinagawa, A. & Seiki, M. (1995) *J. Biol. Chem.* **270,** 23013–23020.
12. Puente, X. S., Pendás, A. M., Liano, E., Velasco, G. & López-Otin, C. (1996) *Cancer Res.* **56,** 944–949.
13. Llano, E., Pendas, A. M., Freije, J. P., Nakano, A., Knauper, V., Murphy, G. & Lopez-Otin, C. (1999) *Cancer Res.* **59,** 2570–2576.
14. Pei, D. (1999) *J. Biol. Chem.* **274,** 8925–8932.
15. d'Ortho, M-P., Will, H., Atkinson, S., Butler, G., Messent, A., Gavrilovic, J., Smith, B., Timpl, R., Zandi, L. & Murphy, G. (1997) *Eur. J. Biochem.* **250,** 751–757.
16. Ohuchi, E., Imai, K., Fujii, Y., Sato H., Seiki, M. & Okada, Y. (1997) *J. Biol. Chem.* **272,** 2446–2451.
17. Apte, S. S., Fukai, N., Beier, D. R & Olsen, B. R., (1997) *J. Biol. Chem.* **272,** 25511–25517.
18. Kinoh, H., Sato, H., Tsunezuka, Y., Takino, T., Kawashima, A., Okada Y. & Seiki, M. (1996) *J. Cell Sci.* **109,** 953–959.
19. Holmbeck, K., Bianco, P., Caterina, J., Yamada, S., Kromer, M., Kuznetsov, S. A., Mankani, M., Robey, P. G., Poole, A. R., Pidoux, I., *et al.* (1999) *Cell* **99,** 81–92.
20. Hiraoka, N., Allen, E., Apel, I. J., Gyetko, M. R. & Weiss. S. J. (1998) *Cell* **95,** 365–377.
21. Young, I. D., Stewart, R. J., Ailles, L., Mackie, A. & Gore, J. (1993) *Biotech. Histochem.* **68,** 153–158.
22. Komminoth, P., Merk, F. B., Leav, I., Wolfe, H. J. & Roth, J. (1992) *Histochemistry* **98,** 217–228.
23. Cao, Y., Linden, P., Farnebo, J., Cao, R., Eriksson, A., Kumar, V., Qi, J-H., Claesson-Welsh, L. & Alitalo, K. (1998) *Proc. Natl. Acad. Sci. USA* **95,** 14389–14394.
24. Cao, Y. & Cao, R. (1999) *Nature (London)* **398,** 381.
25. Knauper, V., Will, H., Lopez-Otin, C., Smith, B., Atkinson, S. J., Stanton, H., Hembry, R. M. & Murphy, G. (1996) *J. Biol. Chem.* **271,** 17124–17131.